

A 2.9-hour periodic radio transient with an optical counterpart

N. HURLEY-WALKER ¹, S. J. MCSWEENEY ¹, A. BAHRAMIAN ¹, N. REA ^{2,3}, C. HORVÁTH ¹, S. BUCHNER ⁴,
A. WILLIAMS ¹, B. W. MEYERS ¹, JAY STRADER ⁵, ELIAS AYDI ⁵, RYAN URQUHART ⁵, LAURA CHOMIUK ⁵,
T. J. GALVIN ^{1,6}, F. COTI ZELATI ^{2,3} AND MATTHEW BAILES ⁷

¹International Centre for Radio Astronomy Research, Curtin University, Kent St, Bentley WA 6102, Australia

²Institute of Space Sciences (ICE), CSIC, Campus UAB, Carrer de Can Magrans s/n, E-08193, Barcelona, Spain

³Institut d'Estudis Espacials de Catalunya (IEEC), Carrer Gran Capità 2–4, E-08034 Barcelona, Spain

⁴South African Radio Astronomy Observatory, 2 Fir Street, Black River Park, Observatory 7925, South Africa

⁵Center for Data Intensive and Time Domain Astronomy, Department of Physics and Astronomy, Michigan State University, East Lansing, MI 48824, USA

⁶CSIRO Space & Astronomy PO Box 1130, Bentley, WA 6102, Australia

⁷Centre for Astrophysics and Supercomputing, Swinburne University of Technology, Mail H30, PO Box 218, VIC 3122, Australia

ABSTRACT

We present a long-period radio transient (GLEAM-X J0704–37) discovered to have an optical counterpart, consistent with a cool main sequence star of spectral type M3. The radio pulsations occur at the longest period yet found, 2.9 hours, and were discovered in archival low-frequency data from the Murchison Widefield Array (MWA). High time resolution observations from MeerKAT show that pulsations from the source display complex microstructure and high linear polarisation, suggesting a pulsar-like emission mechanism occurring due to strong, ordered magnetic fields. The timing residuals, measured over more than a decade, show tentative evidence of a ~ 6 yr modulation. The high Galactic latitude of the system and the M-dwarf star excludes the magnetar interpretation, suggesting a more likely M-dwarf / white dwarf binary scenario for this system.

Keywords: Radio transient sources (2008) — Radio pulsars (1353) – M dwarf stars (982) – Binary stars (154)

1. INTRODUCTION

Transient phenomena are often associated with high-energy or extreme physics, and historically their serendipitous detection has led to new astrophysical advances. In the radio sky, coherent non-thermal emission processes in extreme environments produce transient sources across a range of timescales; the shortest have been mined for pulsars, resulting in the discovery of the millisecond-timescale Fast Radio Bursts (FRBs; Lorimer et al. 2007; Petroff et al. 2022). Slower-timescale (hours to months) coherent emission can be detected from explosive transients such as gamma-ray bursts (van Paradijs et al. 2000) or beamed jets from blazars (Urry & Padovani 1995).

Timescales of minutes to hours have historically been poorly probed. Despite the discovery of GCRT J1745–3009 by Hyman et al. (2005), a radio source that produced five 11-minute duration pulses repeating every 77 minutes, no similar objects were found until the advent of the SKA precursors. Now we are see-

ing an explosion of discovery, with the emerging class of “long-period radio transients” (LPTs)¹.

By searching the GaLactic and Extragalactic All-sky Murchison Widefield Array (MWA; Tingay et al. 2013; Wayth et al. 2018) eXtended (GLEAM-X; Hurley-Walker et al. 2022a) survey at 72–231 MHz using a visibility differencing technique, Hurley-Walker et al. (2022b) discovered the radio transient GLEAM-X J1627–52, which produced ~ 45 -Jy, 30–60 s-wide, highly linearly-polarised pulses every 18 minutes for three months in 2018, with a dispersion consistent with a Galactic origin. This was followed by the discovery of GPM J1839–10, which repeated every 22 minutes, and unlike the previous two very transient sources, was found to be active for at least three decades (Hurley-Walker et al. 2023). Using the Australian SKA Pathfinder (ASKAP) at 888 MHz, Caleb et al. (2024) have discov-

¹ Otherwise called “ultra-long period transients”, “ultra-long period objects”, etc.

ered a $P \sim 54$ -minute transient ASKAP J1935+2148 which produces both broad, linearly-polarised pulses, and short, circularly-polarised bursts. [Dobie et al. \(2024\)](#) have also detected a single 2-minute pulse from ASKAP J1755–25, which phenomenologically resembles the other sources, but has not yet been observed to repeat. [Dong et al. \(2024\)](#) have detected a radio source with $P \sim 421$ s, CHIME J0630+25; at a distance of 170 pc, it is the closest LPT discovered to date, compared to (fairly uncertain) distances of 1–8 kpc for the other sources. [de Ruiter et al. \(2024\)](#) have recently noted linearly-polarised periodic radio emission with a period of ~ 2 hr from a binary M-dwarf / WD system, ILT J1101+5521.

So far, optical association of the LPTs has been difficult, since they have been discovered at low Galactic latitudes in crowded fields. For a few LPTs deep optical and infrared observations were reported. GLEAM-X J1627–52 was observed deeply with large facilities, but its imprecise radio localisation and position in crowded Galactic fields meant that none of the coincident sources could be unambiguously associated, with resulting optical and infrared limits of $g > 23.7$, $i > 22.8$ and $K > 18.2$ magnitude ([Rea et al. 2022](#)). On the other hand, for GPM J1839–10, the 10 m GranTeCan telescope could pinpoint a possible counterpart at its refined radio position with $K_s = 19.7 \pm 0.2$, identified as a main-sequence mid-K or mid-M star (see Methods section in [Hurley-Walker et al. 2023](#)). As for the 54-min source ASKAP J1935+2148, limits of $g > 23.3$, $i > 23.1$, and $y > 21.3$ have been derived ([Caleb et al. 2024](#)). Only for ILT J1101+5521 ([de Ruiter et al. 2024](#)) an optical counterpart could be conclusively pinpointed thus far. In this paper, we present a new LPT, GLEAM-X J0704–37, which has a clear optical counterpart identified with a low-mass star, and might exhibit two long periodicities.

2. OBSERVATIONS AND DATA ANALYSIS

2.1. Identification

Using the MWA, the GLEAM-X survey has observed the sky south of declination $+30^\circ$ in a series of ~ 100 drift scans across 72–231 MHz. Taken at a native time resolution of 0.5 s in two-minute duration snapshots, the data are averaged to 4-s resolution to reduce processing costs. Each snapshot is imaged (with WSCLEAN; [Offringa et al. 2014](#)) to form a deep model of the sky visibilities. Continuum-subtracted images are formed for each 4-s timestep; the resulting cube is then searched with various filters sensitive to pulsed, bursty, or variable emission. We detected the new transient source GLEAM-X J0704–37 as a single 30-s wide pulse in a two-minute

observation on 2018-02-04 at 14:57:02 UT, performed at 103–134 MHz. Searching the archival MWA data back to the commencement of observatory operations in August 2013, we identified 33 further pulses. We found that the shortest interval between consecutive pulses was approximately three hours. Several long-duration drift scans were sensitive to the source’s location, and no pulses were detected at shorter intervals.

2.2. Radio follow-up

We performed follow-up observations with the MeerKAT radio telescope at UHF (550–1050 MHz), using both correlator-mode at 2-s dump times and the Pulsars and Transients User Supplied Equipment (PTUSE [Bailes et al. 2020](#)). In our longest observation, we observed GLEAM-X J0704–37 from 2023-10-04 01:52:32 to 05:57:58, finding two distinct pulses with centroid times of arrival (TOAs) at 02:33:02 and 05:29:59, and no pulses at a shorter interval. The calibrator scans were chosen to be taken at non-integer divisors of the initial period, so that we would not miss any pulsations. We thus confirmed the initial periodicity estimate of ~ 3 hours.

MWA (at 170–200 MHz) and MeerKAT (UHF) conducted a simultaneous observation of a single pulse at 2024-06-05 09:06:48. This enabled a constraint of the radio spectrum between 170 and 1050 MHz, found to be best modelled by a curved power-law of the form:

$$S_\nu = S_{1\text{GHz}} \left(\frac{\nu}{1\text{GHz}} \right)^\alpha \exp q \left(\log \frac{\nu}{1\text{GHz}} \right)^2 \quad (1)$$

with $\alpha = -6.2 \pm 0.6$ and $q = -1.9 \pm 1.4$ (at a reference frequency of 1 GHz). Assuming a distance of 1.5 kpc (Section 2.5), this pulse has a total radio luminosity of $2\Omega_{1\text{GHz}} \times 10^{29} \text{ erg s}^{-1}$, where $\Omega_{1\text{GHz}}$ is the beam solid angle at 1 GHz.

The TOAs of individual pulses were determined using the same method as described by [Hurley-Walker et al. \(2023\)](#). The timing residuals (Fig. 1) demonstrate an additional sinusoidal variation of the radio emitter. A timing analysis for 2013–2020 yields a period of $P = 10496.5575 \pm 0.0005$ s, a period derivative of $< 1.3 \times 10^{-11} \text{ s s}^{-1}$, and this additional modulation at $P_{\text{long}} = 2,283 \pm 84$ days. The spin-down rate \dot{P} should be considered as an upper limit given that its error encapsulates zero spin-down (see bottom panel of Fig. 1).

Following the method of [Erkut \(2022\)](#), we choose a conservative 3σ upper limit of $\dot{P} < 3.9 \times 10^{-11} \text{ s s}^{-1}$, and thereby derive a beam solid angle of $\Omega_{1\text{GHz}} < 1.5 \times 10^{-5}$, consistent with the short pulse duty cycle (~ 30 – 60 s in 2.9 hr). This produces a radio luminosity limit of $\lesssim 3 \times 10^{25} \text{ erg s}^{-1}$; pulses up to $20\times$ brighter are also

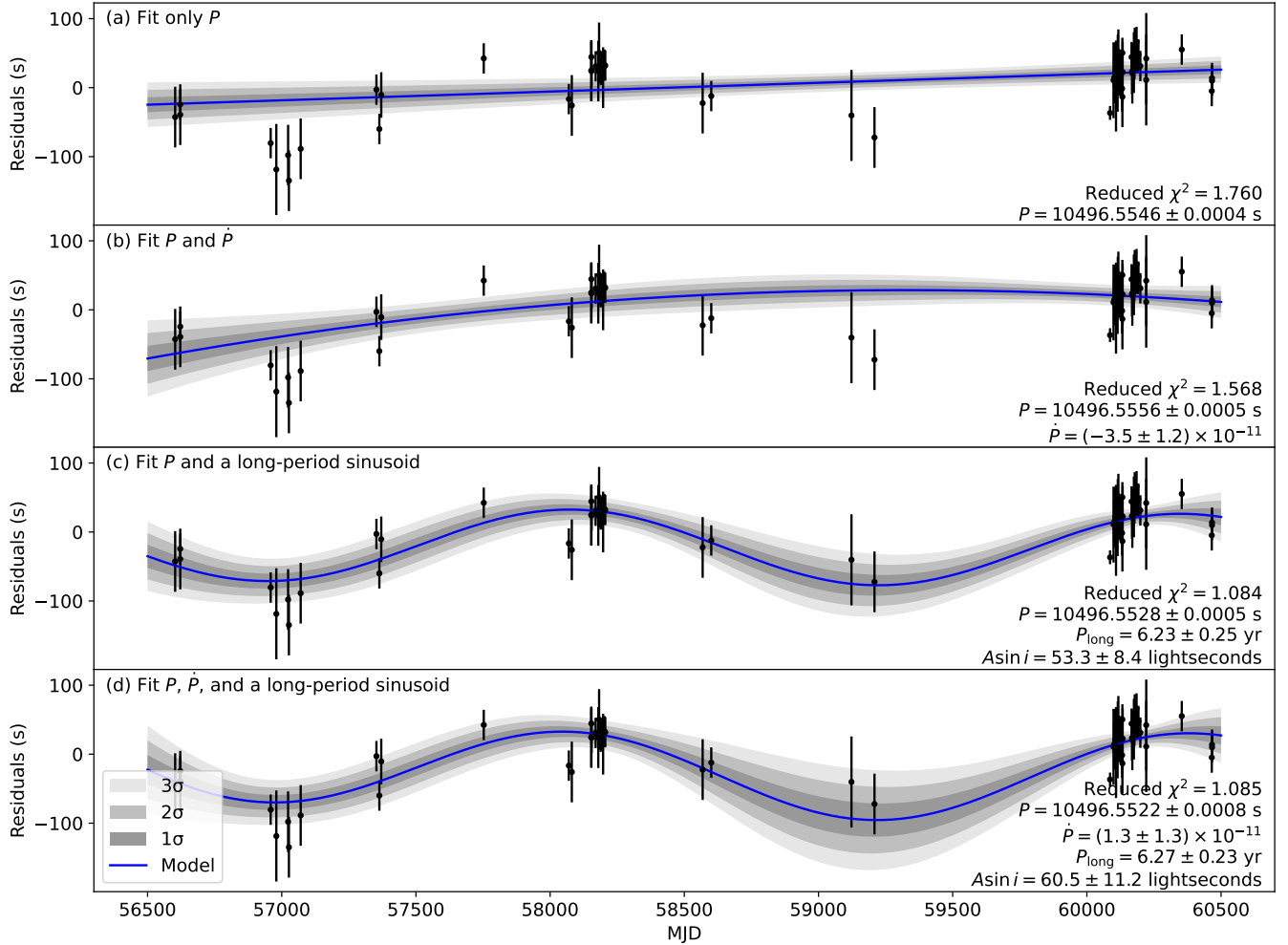


Figure 1. Various model fits to the timing residuals assuming an initial folding period of 10496.5531 s. The fitted parameters are: P , the rotation period; \dot{P} , the spindown rate; P_{long} , a sinusoidal period; and $Asin i$, the sinusoidal amplitude projected onto the line of sight. Reported errors are 1- σ . The fit that includes only P and \dot{P} (b) produces a non-physical (negative) spin down. The fits with P_{long} (c & d) are favoured over those without (a & b).

observed. No secular change in brightness with respect to time has been observed, after correcting the MWA and MeerKAT data to the same frequency.

To measure the position, the MeerKAT correlator data at the time intervals covering the brightest seven pulses were imaged. The position measurements showed variance beyond that which would be expected from thermal noise, implying small ($\sim 0.5''$) phase-referencing (astrometric) errors which vary between observations, consistent with expected variations from ionospheric refractive shifts. We thus derive the position from the average of the position measurements, and the error by the standard deviation: in J2000, RA=07^h04^m13.^s19 and Dec=−37°06′14″.3, with a (1- σ) uncertainty of 0″.3.

No persistent radio source was detected down to a 3σ limit of $30 \mu\text{Jy beam}^{-1}$ using MeerKAT UHF data integrated outside of the pulse activity windows.

Smaller timescales were probed with the PTUSE data, which has a native time resolution of $\sim 10 \mu\text{s}$. We discovered abrupt changes in the brightness in both the precursor emission (at ~ 300 s in panel (a) of Fig. 2) as well as in the bright peak (at ~ 340 s). Such changes were predominantly in the form of narrow peaks, $\lesssim 10$ ms in width, but also occasionally appear as similarly sized *reductions* in brightness (in particular panel (c) of Fig. 2). Although the PTUSE data also showed some instrumental gain changes (whose origin remains unclear), these could be distinguished from the abrupt brightness changes of GLEAM-X J0704–37 by virtue of the astrophysical dispersion of the intrinsic emission, corresponding to a dispersion delay of $\tau_{\text{DM}} \approx 0.4$ s across the observing band. This microstructure enabled a highly accurate calculation of the dispersion measure: $36.541 \pm 0.005 \text{ pc cm}^{-3}$.

After correcting for dispersion and frequency-scrambling, the resulting light curve, shown in panel (c) of Fig. 2, has effectively had all instrumental gain changes (at all timescales) removed, and retains only brightness variations of GLEAM-X J0704–37 smaller than τ_{DM} . The ACF analysis of the cleaned PTUSE lightcurve (and a few representative subsections of it) is shown in panel (d). Only in one section, corresponding to the trailing side of the brightest peak, did we find clear evidence of a quasi-periodicity of ~ 40 ms; elsewhere, we did not detect any significant periodicity.

The radio polarisation behaviour of the source is extremely complex, with strong linear (20–50 %) and some circular polarisation (10–30 %) that changes on short (ms) timescales. This behaviour is in contrast with the high (95 %) linear polarisation and flat polarisation angles observed in GLEAM-X J1627, and bears some similarity to the complex behaviour recently uncovered in GPM J1839–10 (Men et al. 2024, in press). A companion paper, McSweeney et al. in preparation, discusses the polarisation behaviour of all three sources in more detail. For those parts of the brightest pulses where the Faraday rotation is clear, we derive a rotation measure of $-7 \pm 1 \text{ rad m}^{-2}$.

2.3. Optical & Infrared counterpart

We inspected and analyzed archival images and catalogs covering the region, including images by the Dark Energy Camera at the Blanco 4m telescope at the Cerro Tololo Inter-American Observatory in Chile (Flaugher et al. 2015), and catalogs from Gaia Data Release 3 (Gaia DR3; Gaia Collaboration et al. 2023) and the VISTA Hemisphere Survey (VHS; McMahon et al. 2013). We identified an optical counterpart $0''.3$ away from the MeerKAT localization (Fig. 3; left) with Gaia designation of Gaia DR3 5566254014771398912 and coordinates of RA= $07^{\text{h}}04^{\text{m}}13.^{\text{s}}19$, Dec= $-37^{\circ}06'14''58$, with uncertainties of 0.8 and 1 milliarcseconds in RA and Dec, respectively. Considering the stellar density in this region in Gaia DR3, we estimated the probability of a chance alignment with a separation of $\leq 0''.3$ to be 0.05%.

We performed spectroscopy of this optical counterpart with the Goodman Spectrograph (Clemens et al. 2004) on the SOAR telescope on 2023 October 25 with a 400 line mm^{-1} grating and a $1.2''$ -longslit, yielding a FWHM resolution of 6.7 \AA over a wavelength range of $4000\text{--}7840 \text{ \AA}$. Two 30-min exposures were taken, for a total exposure time of 1 hr. The data were reduced, optimally extracted, and combined in the normal manner in IRAF (Tody 1986).

The SOAR spectrum shows significant molecular lines, such as TiO absorption features (Fig. 3; right), consistent with M stars. Comparing with PHOENIX spectral models (Husser et al. 2013) and X-shooter spectral library DR3 (Verro et al. 2022), we inferred a spectral type of M3 with a temperature of $\sim 3400 \text{ K}$. Combined with the constraints on the distance (see §2.5) and apparent brightness of the source, which rules out a red giant, we conclude that the optical source is an M3V star. In Fig. 3 (right) we also show the comparison with a WD+M3V system with a WD with $T = 11,500 \text{ K}$ and $M = 0.8 M_{\odot}$ (like AR Sco), showing that a WD star would not be detectable.

2.4. X-ray observations

We observed GLEAM-X J0704–37 using XMM-Newton beginning on November 16, 2023, at 23:07 UT and ending on November 17, 2023, at 09:02 UT. This time span overlapped with a 7-hour dwell starting on November 17th at 01:20 UT on the MeerKAT telescope (in UHF). All European Photon Imaging Camera (EPIC) cameras were set to Full-Frame mode.

The data were processed using the Science Analysis System (SAS version 21.0; Gabriel et al. 2004). The data were significantly affected by strong background flares. After removing these flares, the usable data was reduced to $\simeq 15.2 \text{ ks}$ for EPIC-pn and $\simeq 16.2 \text{ ks}$ for the EPIC-MOSs. No X-ray source was detected at the position of GLEAM-X J0704–37. We estimated the $3\text{-}\sigma$ upper limit on the EPIC-pn net count rate at the source position to be $2 \times 10^{-3} \text{ counts s}^{-1}$ over the $0.3\text{--}10 \text{ keV}$ energy range. This results in a $3\text{-}\sigma$ upper limit on the unabsorbed flux of $\sim 9 \times 10^{-15} \text{ erg s}^{-1} \text{ cm}^{-2}$ assuming a power law spectrum with a photon index of $\Gamma = 2$, or $\sim 5 \times 10^{-15} \text{ erg s}^{-1} \text{ cm}^{-2}$ assuming a black body spectrum with a temperature of $kT=0.3 \text{ keV}$. In both cases, we accounted for the effects of absorption by the interstellar medium by incorporating the TBABS absorption component (Wilms et al. 2000) into the model, adopting a hydrogen column density of $N_H = 2.7 \times 10^{21} \text{ cm}^{-2}$ (this is the expected value along the line of sight to the source within our Galaxy; Willingale et al. 2013). Combined with the constraints on the distance (see §2.5) these limits convert to a luminosity of $L_X < 2.2 \times 10^{30} \text{ erg s}^{-1}$ for the assumed power-law spectrum and $L_X < 1.1 \times 10^{30} \text{ erg s}^{-1}$ for the black body case.

During the time XMM-Newton/EPIC was on source, two radio bursts were detected with MeerKAT, at 2023-11-17T02:01:25 and 04:56:29 (UTC). We shifted the X-ray and radio time stamps to the Solar System’s barycenter, using the radio position and the DE-430 JPL ephemeris for reference, and extracted images from

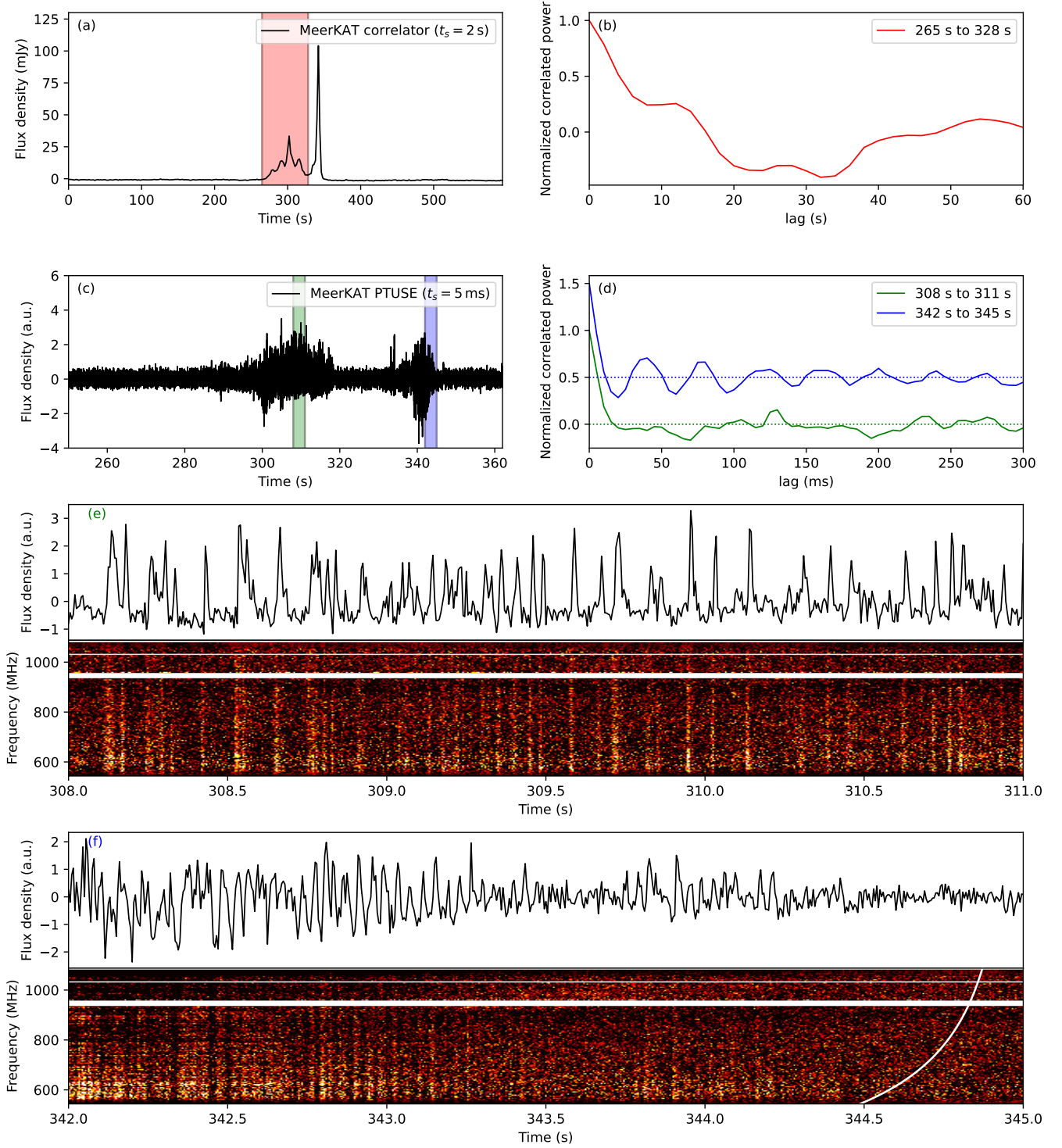


Figure 2. Autocorrelation analysis of both the correlator lightcurve sampled at 2 s (a & b) and the PTUSE lightcurve sampled at 5 ms (c & d), and subsets of the PTUSE data with significant microstructure (e & f). The autocorrelations in (b) & (d) include only the corresponding data highlighted in panels (a) & (c); a vertical offset has been applied to the blue curve in panel (d) for visual clarity. The preprocessing of the PTUSE data (see main text) has effectively removed variations on timescales $\gtrsim 0.4$ s, but retains finer time structures. In at least one section (colored blue, with detail shown in panel (f)), a quasi-periodicity of ~ 40 ms is clearly evident. The dynamic spectra have been dedispersed to $36.541 \text{ pc cm}^{-3}$. In panel (f), a white curve indicates how a zero-DM transient signal would appear.

various time intervals around these bursts. No excess emission was detected above the background level. We measured upper limits on the EPIC-pn net count rate within a 100-s time window centered on the times of the two bursts, yielding values of $0.09 \text{ counts s}^{-1}$ and $0.06 \text{ counts s}^{-1}$, respectively ($3\text{-}\sigma$; 0.3–10 keV). Assuming the same spectral models as those used for the average emission, the corresponding luminosity limits are $L_{X,PL} < 1.1 \times 10^{32} \text{ erg s}^{-1}$ and $L_{X,BB} < 6.6 \times 10^{31} \text{ erg s}^{-1}$ for the first burst and $L_{X,PL} < 7.3 \times 10^{31} \text{ erg s}^{-1}$ and $L_{X,BB} < 4.4 \times 10^{31} \text{ erg s}^{-1}$ for the second burst.

2.5. Distance

We can convert our accurate estimate of the dispersion measure (Section 2.2) into a distance using electron density models of the Milky Way. Depending on the model used, the resulting estimated distance is $0.4(\pm 0.1)$ (YMW16; Yao et al. 2017) or $1.8(\pm 0.5)$ kpc (NE2001; Cordes 2004).

We may also estimate the distance using the parallax measured by the *Gaia* mission (Gaia Collaboration et al. 2016). *Gaia* DR3 reports a parallax of -0.22 ± 1.0 mas, indicating that any inference of distance would be heavily reliant on prior models (e.g., Hogg 2018). We estimated the distance using the Bailer-Jones et al. (2018) geometric model based on stellar distributions and found a value of $2.5^{+1.5}_{-0.9}$ kpc. Considering the optical spectrum, and comparing with dereddened spectra of nearby red dwarfs, we estimated $E(B - V) = 0.2$, which in the context of Galactic extinction maps (Green 2018; Edenhofer et al. 2024) suggests a distance of $\gtrsim 1$ kpc. Combining these constraints, we assume a distance of 1.5 ± 0.5 kpc throughout the remainder of the paper, but we note that this is significantly uncertain.

3. DISCUSSION

The discovery of linearly-polarised, $P = 2.9$ -hour pulses from GLEAM-X J0704–37 places it in the burgeoning class of “long-period radio transients”. We have identified an optical counterpart for an LPT, with a clear M3-dwarf spectrum. The radio luminosity of the periodic bursts are as high as $\sim 10^{29} \text{ erg s}^{-1}$, while at X-ray energies the bursts are found to be fainter than $L_X \sim 10^{32} \text{ erg s}^{-1}$.

The radio emission shows microstructures and a peculiar long-period timing modulation of ~ 6 yr. It is tempting to interpret P_{long} as an orbital period of a system composed of an M-dwarf and a 2.9 hr spinning NS or a WD (see also below). However it is possible that the long-term variation in timing residuals is due to a stochastic, red process analogous to timing noise in canonical pulsars, whose physical origins are still un-

known. Assuming a simple period-only model, the amplitude of our residuals is ± 50 s, i.e. an amplitude of 1% of the spin period, and only a factor of a few larger than the pulse width. If we assume most of the power in the residuals is near the best-fitting frequency of $1/P_{\text{long}} \approx 0.16 \text{ yr}^{-1}$, then we can compare, to first order, the implied power spectral density of the TOA residuals to the pulsars studied by Parthasarathy et al. (2019), who characterise timing noise as a power-law power spectrum. We find that the power spectral density of GLEAM-X J0704–37 significantly exceeds that of the pulsars in their sample (extrapolated to the same frequency). It remains unclear how (or even if) GLEAM-X J0704–37’s vastly larger period might affect this kind of timing noise.

It is also worth noting that ascribing the absolute peak-to-peak amplitude of ~ 100 s to a change in the compact object’s angular momentum implies a phenomenal transfer of energy, regardless of whether the compact object is a NS or a WD, and they are more likely to arise from changes in the emission region than in glitches of the rotator.

Below we discuss several possibilities starting from the firm detection of periodic radio pulses and the M-dwarf optical spectrum of the counterpart.

3.1. Stellar radio flares or exo-planet interaction?

The presence of an M-dwarf coincident with the radio emission is unseen in other long-period radio transients. Radio emission from stars is typically circularly polarized, and appears in flares or bursts due to sunspot activity (Dulk 1985; Lynch et al. 2017) or, potentially detectable at low radio frequencies (< 200 MHz), star–exo-planet interactions (Vedantham et al. 2020). Such flares would be wholly undetectable at 10^2 – 10^3 pc, and the strong periodicity is also difficult to explain with a purely stellar origin. The closest analogue is CU Virginius, a hot, magnetic chemically-peculiar, Ap-type star 72 pc away, which has been observed to produce pulses of 100%-circularly-polarised emission at 1–3 GHz, each lasting an hour, and repeating every 12 hours, the rotation rate of the star (Lo et al. 2012). These are thought to be produced from electron cyclotron maser emission in the magnetosphere of the star. The high linear polarisation fraction (up to 50%) of GLEAM-X J0704–37 would be difficult to explain with this emission mechanism. Das & Chandra (2021) observed pulsations from CU Virginius of brightnesses up to 100 mJy at 1–2 GHz; even these are ~ 400 times less luminous than the brightest pulses from GLEAM-X J0704–37.

We therefore exclude the possibility that the M-dwarf alone produces the radio emission, and conclude that it

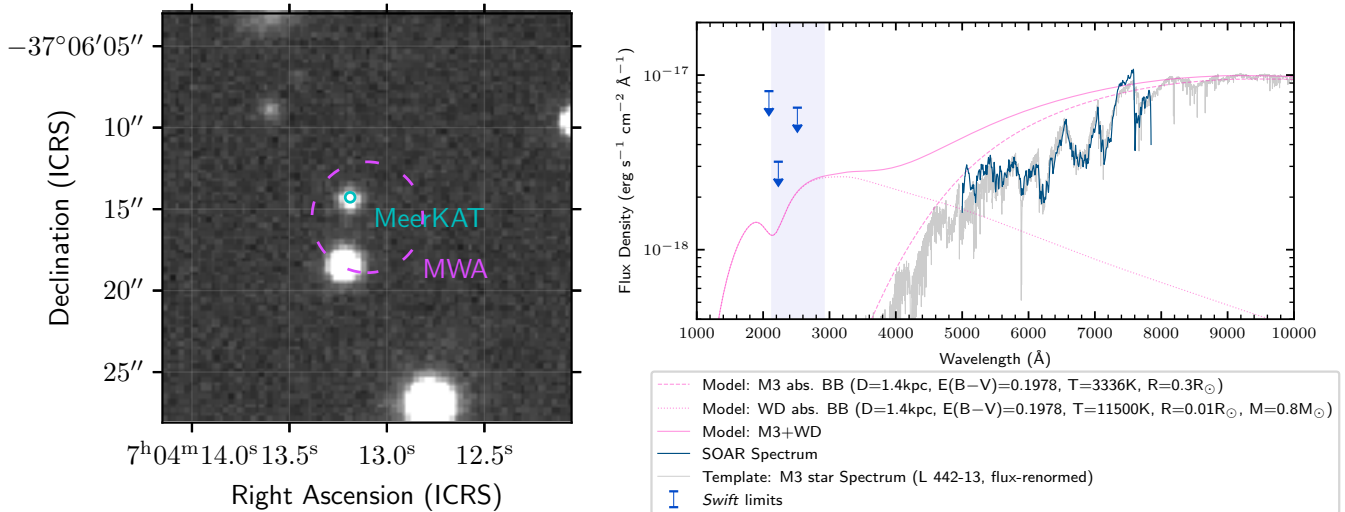


Figure 3. Left: DECAM r-band image of the vicinity of the radio transient, with its $1\text{-}\sigma$ localization regions by MWA (dashed magenta circle) and MeerKAT (solid cyan circle) overlaid. Right: SOAR (4m-class) low-resolution optical spectrum of the optical counterpart (blue solid line) overlaid on an example M3V star (grey line, flux and extinction renormalized to match). The *Swift*-UVOT limits are shown with downward-pointing arrows. An AR Sco-like WD with $T = 11,500\text{ K}$, $M = 0.8M_{\odot}$ is shown with the dotted pink line, and the summed WD+M3V spectrum is shown with a solid pink line.

is in a binary orbit with an as-yet optically undetected radio emitter.

3.2. A binary system with a neutron star

Since the optical spectrum shows no evidence of a further main-sequence companion (Fig. 3), we suggest that the radio emitter is a compact stellar remnant. The high linear polarisation suggests ordered magnetic fields. Therefore, the companion is likely to be an NS or WD. In both cases, periodic radio emission might be generated, although not all the observational properties of GLEAM-X J 0704–37 are easily interpreted.

In the NS case, the high Galactic latitude of the system ($|b| = 13^{\circ}$), the M-dwarf companion and the faint X-ray emission argue against a magnetar companion. These young NSs are generally isolated, often lie within massive star clusters or supernova remnants, and field decay exponentially dissipates their surface magnetic energy on Myr timescales (Viganò et al. 2013). This time is too short to allow them to leave the plane of the Galaxy even for extreme proper motions. If this source is a NS / M-dwarf binary, it is necessarily an old pulsar with a relatively low B field. Many such systems are known in different evolutionary stages, from radio-emitting millisecond pulsars (Lorimer 2008) to accreting low-mass x-ray binaries (Bahramian & Degenaar 2023) or transitional systems (Papitto & de Martino 2022). However in all such cases the pulsar has undergone a recycling period due to accretion from the companion star spinning very fast, with usually hours-timescale orbits. For an NS pulsar binary to have a 2.9 hr spin period while

still maintaining enough magnetic field strength or rotational energy to produce radio pulsations, the NS must have been accreting in the propeller regime for an extended period. This process would gradually slow its rotation while preserving its magnetic field, but would require very fine-tuned conditions. Even then, the magnetic field necessary to power the current radio emission (which would have to be spin-down-powered in this case) would exceed 10^{17} G , which is unrealistically large given the NS old age. Therefore, if this system is indeed a NS binary with a 2.9-hour spin period, it would challenge our current understanding of NS accretion and magnetic field evolution. Alternatively, interpreting the 2.9-hour periodicity as an orbital period introduces more challenges, since the radio transient nature of the system, micro-structures and small duty cycle are difficult to explain through geometric considerations.

Kramer et al. (2024) analysed the quasi-periodicity microstructure timescale P_{μ} of NS pulsations across six orders of magnitude of rotational period, finding a universal relation of $P_{\mu} = A_P P^{\gamma}$ ms, with $A_P = 1.12 \pm 0.14$ and $\gamma = 1.03 \pm 0.04$. This would predict $P_{\mu} = 15.5\text{ s}$ for GLEAM-X J 0704–37. Most pulses detected with MeerKAT are about 80 s wide without much distinct substructure visible above the noise. In Fig. 2 we present the brightest detected pulse, and an auto-correlation analysis on data from both the correlator (timescales 2 s–120 s) and PTUSE (1 ms–400 ms). Intermediate timescales were contaminated with instrumental artefacts, likely from the PTUSE gain calibration. On the longer timescales, we see a peak in the ACF at

12 s, broadly consistent with the Kramer et al. prediction.

The detected timescale of $40 \text{ ms} \approx 4 \times 10^{-6}$ periods is much shorter than the Kramer et al. (2024) relation, but can be compared to the spacing of nanoshots observed in the Crab pulsar, $\lesssim 0.1 \mu\text{s} \approx 3 \times 10^{-6}$ periods (cf. Hankins & Eilek 2007, Fig. 3). However, examples of known nanostructure are rare, and there is no universal relation for nanostructure analogous to the microstructure relation discussed above, so it would be premature to conjecture that the physical cause of the fine structure of GLEAM-X J0704–37 is in any way related to that of the Crab nanoshots. The behavior of the fine structure is also comparable to that of PSR J0901–4046 (Caleb et al. 2022, esp. Extended Data Fig. 2), whose ACFs indicate quasi-periodicities on similar timescales (i.e. tens of milliseconds), even though the ratio of the quasi-periodic timescale to the rotation period is two orders of magnitude larger than for GLEAM-X J0704–37.

3.3. A binary system with a white dwarf

Another possibility is that the compact object in the binary system is a WD, presumably with a strong magnetic field. In polars, a type of magnetic cataclysmic variable (MCV), the magnetic field of the white dwarf is 10–200 MG, and the two stars are locked in synchronous rotation. Intermediate polars have slightly weaker magnetic fields (1–10 MG); the WD rotates at a faster rate than the orbit. With an even faster WD rotation rate, AR Sco-type systems consist of an M-dwarf/WD pair in a tight (~ 4 -hr) orbit, such that the M-dwarf is nearly Roche-lobe filling (Marsh et al. 2016). Interactions between the two stars cause pulsar-like radio emission from the magnetosphere of the WD, which has been directly observed in J1912-44, as the beam of the WD crosses our line-of-sight (Pelisoli et al. 2023). The two known “WD pulsar” systems were selected by looking for high optical variability, which preferentially selects for nearby systems with quickly-spinning WDs ($P_{\text{spin}} \sim$ minutes). It is therefore possible that slowly-rotating AR Sco-type systems could have been missed by optical searches. The observed periodicity of 2.9 hr is however consistent with the rotation rate of the WDs in the MCV population (Norton et al. 2004).

The recently discovered ILT J1101+5521 de Ruiter et al. (2024), a ~ 2 hr synchronized polar system composed by a WD and an M-dwarf showing periodic and coherent radio emission, might be a twin system with GLEAM-X J0704–37. In this scenario, the 2.9 hr periodicity might be interpreted as both the spin and the orbital period, and the ~ 6 yr modulation either as timing noise or as a possible super-orbital modulation.

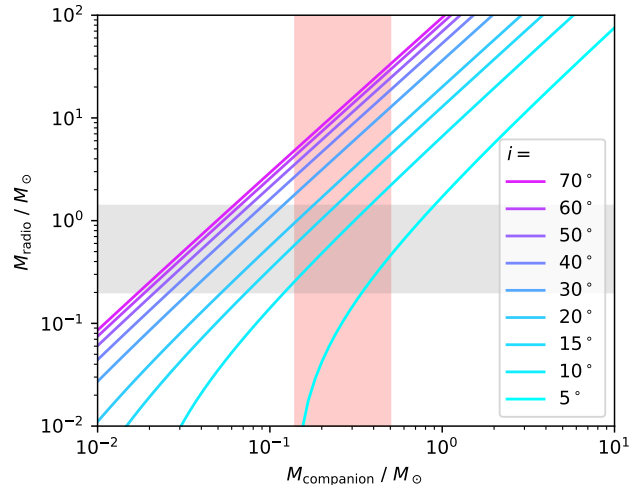


Figure 4. Allowable inclination angles i for a circular orbit with period $P_{\text{long}} = 2,283$ day of an unseen radio emitter and the visible M3 dwarf. The grey shaded area shows the mass range of magnetic white dwarfs (Amorim et al. 2023) and the red shaded area shows the mass range of M3V dwarfs (Cifuentes et al. 2020). For an MCV interpretation, a low inclination angle is preferred.

The UV limits derived by a 3 ks of *Swift* observations yielded upper limits on the UV/blue emission, shown in Fig. 3. This rules out the presence of WDs with $T \gtrsim 13,000$ K, i.e. about 44% of the magnetic WD population. However, the WDs in J1912-44, AR Sco and ILT J1101+5521 are all cooler, with the latter having a temperature of $T_{\text{eff}} \sim 5156$ K (de Ruiter et al. 2024). Sensitive observations below a wavelength of 400 nm are required.

In the hypothesis of the long ~ 6 yr periodicity being instead the orbit of the system, the small amplitude of the timing residuals (± 50 s) implies a very low inclination angle (Fig. 4). The beam opening angle of this system would then be extremely small, just $\sim 30 \text{ s} / 10,000 \text{ s} \sim 0.6\%$. If past accretion from the stellar companion has aligned the rotation and orbital axes, as is common in MCVs, then the radio beam would also be nearly aligned with the WD rotation axis. This would then present a selection effect: radio searches will tend to find systems with small inclination angles.

Assuming an M3V stellar mass of $0.32M_{\odot}$ and a WD mass of $0.8M_{\odot}$, the Roche lobe radius of the M3V star is 0.2 A.U. For $i = 10^{\circ}$, and a circular 2,283 day orbit, the distance between the two sources would be 2.4 A.U. So, potentially, rather than an AR Sco type scenario with a close-by interaction, or a polar-like system as ILT J1101+5521, the pulsar emission is instead generated by a stellar wind flowing from the M-dwarf com-

panion onto the magnetosphere of the WD, where it is accelerated, producing radio emission.

4. CONCLUSION

We have discovered a new long-period radio transient with the longest period yet detected (2.9 hr), and an optical counterpart with an M-dwarf spectrum. In this discovery paper we argue that:

1. The radio emission does not arise purely from the M-dwarf, and the system is most likely a binary with an unseen radio emitter, probably a neutron star or relatively cool magnetic white dwarf;
2. A binary system with an M-dwarf/neutron star is disfavoured by several arguments. If the radio emission is produced by a strong magnetic field, the hosted NS should be young, which is disfavoured by the high Galactic latitude. On the other hand, a scenario with a low-field NS in a low-mass binary (like the transitional pulsars or recycled pulsars), with the radio emission being dipolar spin-down powered, is disfavoured since the radio luminosity is several orders of magnitude larger than the limits on the spin-down.
3. A binary system with an M-dwarf/white dwarf is a viable scenario. The radio emission in this case should be generated by a stellar wind flowing from the M-dwarf companion onto the magnetosphere of the white dwarf, where it is accelerated, producing radio emission. If this can be confirmed, these systems can be evolutionarily connected to AR Sco-type systems, intermediate polars, and polar WDs. A similar system might be the radio emitting polar candidate ILT J1101+5521 (de Ruiter et al. 2024).
4. The microstructure in the radio pulses is consistent with the relationship seen in neutron stars (Kramer et al. 2024), but finer-timescale (~ 40 -ms) nanostructure is observed, whose origin is unknown; it is still unclear how these microstructures behave in radio-emitting WD binaries.
5. There is tentative evidence for a ~ 6 years periodicity possibly due to timing noise. If interpreted as an orbital period, it would place the source an order of magnitude too far apart to be interacting in a similar manner to AR Sco-type or ILT J1101+5521 systems. Furthermore, an M-dwarf/WD binary system with such a long orbital period would be challenging to form an evolutionary perspective. More data are needed to disentangle the nature of this long-timescale periodicity.

To conclusively determine the nature of this system, we suggest further radio monitoring to constrain the timing, sensitive blue/UV observations to search for a WD, and a measurement of the radial velocity of the M-dwarf by studying Doppler shifts of its spectral lines. Determining the nature of this system would be a further step in assessing the true nature of the enigmatic long-period radio transients.

This scientific work uses data obtained from Inyarrimanha Ilgari Bundara / the Murchison Radio-astronomy Observatory. We acknowledge the Wajarri Yamaji People as the Traditional Owners and native title holders of the Observatory site. This work was supported by resources provided by the Pawsey Supercomputing Research Centre’s Setonix Supercomputer (<https://doi.org/10.48569/18sb-8s43>). The Murchison Radio-astronomy Observatory and the Pawsey Supercomputing Research Centre are initiatives of the Australian Government, with support from the Government of Western Australia and the Science and Industry Endowment Fund. Support for the operation of the Murchison Widefield Array is provided by the Australian Government (NCRIS), under a contract to Curtin University administered by Astronomy Australia Limited. The authors would like to thank SARAO for the approval of the MeerKAT DDT request DDT-20230529-NH-01. The MeerKAT telescope is operated by the South African Radio Astronomy Observatory, which is a facility of the National Research Foundation, an agency of the Department of Science and Innovation (DSI). This research is based on observations obtained with *XMM-Newton*, an ESA science mission with instruments and contributions directly funded by ESA Member States and NASA. We thank N. Schartel for approving our DDT request and the *XMM-Newton* Science Operations Centre for carrying out the observation. Based in part on observations obtained at the Southern Astrophysical Research (SOAR) telescope, which is a joint project of the Ministério da Ciência, Tecnologia e Inovações (MCTI/LNA) do Brasil, the US National Science Foundation’s NOIRLab, the University of North Carolina at Chapel Hill (UNC), and Michigan State University (MSU). N.H.-W. is the recipient of an Australian Research Council Future Fellowship (project number FT190100231). N. R. is supported by the European Research Council (ERC) via the Consolidator Grant “MAGNESIA” under grant agreement No. 817661 and from an ESA Science Faculty Visitor program to ESTEC (funding reference ESA-SCI-E-LE-054). F. C. Z. is supported by a Ramón y Cajal fellowship (grant agreement RYC2021-030888-I). N. R. and F. C. Z. acknowledge support from the Catalan grant SGR2021-01269 and by the program Unidad de Excelencia María de Maeztu CEX2020-001058-M. C. H. acknowledges a Doctoral Scholarship and an Australian Government Research Training Programme scholarship administered through Curtin University of Western Australia. J.S. acknowledges support from the Packard Foundation and National Science Foundation (NSF) grant AST-2205550. L.C. is grateful for support from NSF grants AST-2107070 and AST-2205628 and NASA grant 80NSSC23K0497. E.A. acknowledges support by NASA through the NASA Hubble Fellowship grant HST-HF2-51501.001-A awarded by the Space Telescope Science Institute, which is operated by the Association of Universities for Research in Astronomy, Inc. for

REFERENCES

- Amorim, L. L., Kepler, S. O., Külebi, B., Jordan, S., & Romero, A. D. 2023, *ApJ*, 944, 56, doi: [10.3847/1538-4357/acaf6e](https://doi.org/10.3847/1538-4357/acaf6e)
- Bahramian, A., & Degenaar, N. 2023, in *Handbook of X-ray and Gamma-ray Astrophysics* (Springer Singapore), 120, doi: [10.1007/978-981-16-4544-0_94-1](https://doi.org/10.1007/978-981-16-4544-0_94-1)
- Bailer-Jones, C. A. L., Rybizki, J., Fouesneau, M., Mantelet, G., & Andrae, R. 2018, *AJ*, 156, 58, doi: [10.3847/1538-3881/aacb21](https://doi.org/10.3847/1538-3881/aacb21)
- Bailes, M., Jameson, A., Abbate, F., et al. 2020, *PASA*, 37, e028, doi: [10.1017/pasa.2020.19](https://doi.org/10.1017/pasa.2020.19)
- Caleb, M., Heywood, I., Rajwade, K., et al. 2022, *Nature Astronomy*, 6, 828, doi: [10.1038/s41550-022-01688-x](https://doi.org/10.1038/s41550-022-01688-x)
- Caleb, M., Lenc, E., Kaplan, D. L., et al. 2024, *Nature Astronomy*, doi: [10.1038/s41550-024-02277-w](https://doi.org/10.1038/s41550-024-02277-w)
- Cifuentes, C., Caballero, J. A., Cortés-Contreras, M., et al. 2020, *A&A*, 642, A115, doi: [10.1051/0004-6361/202038295](https://doi.org/10.1051/0004-6361/202038295)
- Clemens, J. C., Crain, J. A., & Anderson, R. 2004, in *Society of Photo-Optical Instrumentation Engineers (SPIE) Conference Series*, Vol. 5492, *Ground-based Instrumentation for Astronomy*, ed. A. F. M. Moorwood & M. Iye, 331–340, doi: [10.1117/12.550069](https://doi.org/10.1117/12.550069)
- Cordes, J. M. 2004, in *Astronomical Society of the Pacific Conference Series*, Vol. 317, *Milky Way Surveys: The Structure and Evolution of our Galaxy*, ed. D. Clemens, R. Shah, & T. Brainerd, 211
- Das, B., & Chandra, P. 2021, *ApJ*, 921, 9, doi: [10.3847/1538-4357/ac1075](https://doi.org/10.3847/1538-4357/ac1075)
- de Ruiter, I., Rajwade, K. M., Bassa, C. G., et al. 2024, *arXiv e-prints*, arXiv:2408.11536, doi: [10.48550/arXiv.2408.11536](https://doi.org/10.48550/arXiv.2408.11536)
- Dobie, D., Zic, A., Oswald, L. S., et al. 2024, *arXiv e-prints*, arXiv:2406.12352, doi: [10.48550/arXiv.2406.12352](https://doi.org/10.48550/arXiv.2406.12352)
- Dong, F. A., Clarke, T., Curtin, A. P., et al. 2024, *arXiv e-prints*, arXiv:2407.07480, doi: [10.48550/arXiv.2407.07480](https://doi.org/10.48550/arXiv.2407.07480)
- Dulk, G. A. 1985, *ARA&A*, 23, 169, doi: [10.1146/annurev.aa.23.090185.001125](https://doi.org/10.1146/annurev.aa.23.090185.001125)
- Edenhofer, G., Zucker, C., Frank, P., et al. 2024, *A&A*, 685, A82, doi: [10.1051/0004-6361/202347628](https://doi.org/10.1051/0004-6361/202347628)
- Erkut, M. H. 2022, *MNRAS*, 514, L41, doi: [10.1093/mnras/514/l41](https://doi.org/10.1093/mnras/514/l41)
- Flaugher, B., Diehl, H. T., Honscheid, K., et al. 2015, *AJ*, 150, 150, doi: [10.1088/0004-6256/150/5/150](https://doi.org/10.1088/0004-6256/150/5/150)
- Gabriel, C., Denby, M., Fyfe, D. J., et al. 2004, in *Astronomical Society of the Pacific Conference Series*, Vol. 314, *Astronomical Data Analysis Software and Systems (ADASS) XIII*, ed. F. Ochsenbein, M. G. Allen, & D. Egret, 759
- Gaia Collaboration, Prusti, T., de Bruijne, J. H. J., et al. 2016, *A&A*, 595, A1, doi: [10.1051/0004-6361/201629272](https://doi.org/10.1051/0004-6361/201629272)
- Gaia Collaboration, Vallenari, A., Brown, A. G. A., et al. 2023, *aap*, 674, A1, doi: [10.1051/0004-6361/202243940](https://doi.org/10.1051/0004-6361/202243940)
- Green, G. 2018, *The Journal of Open Source Software*, 3, 695, doi: [10.21105/joss.00695](https://doi.org/10.21105/joss.00695)
- Hankins, T. H., & Eilek, J. A. 2007, *ApJ*, 670, 693, doi: [10.1086/522362](https://doi.org/10.1086/522362)
- Hogg, D. W. 2018, *arXiv e-prints*, arXiv:1804.07766, doi: [10.48550/arXiv.1804.07766](https://doi.org/10.48550/arXiv.1804.07766)
- Hurley-Walker, N., Galvin, T. J., Duchesne, S. W., et al. 2022a, *PASA*, 39, e035, doi: [10.1017/pasa.2022.17](https://doi.org/10.1017/pasa.2022.17)
- Hurley-Walker, N., Zhang, X., Bahramian, A., et al. 2022b, *Nature*, 601, 526, doi: [10.1038/s41586-021-04272-x](https://doi.org/10.1038/s41586-021-04272-x)
- Hurley-Walker, N., Rea, N., McSweeney, S. J., et al. 2023, *Nature*, 619, 487, doi: [10.1038/s41586-023-06202-5](https://doi.org/10.1038/s41586-023-06202-5)
- Husser, T. O., Wende-von Berg, S., Dreizler, S., et al. 2013, *A&A*, 553, A6, doi: [10.1051/0004-6361/201219058](https://doi.org/10.1051/0004-6361/201219058)
- Hyman, S. D., Lazio, T. J. W., Kassim, N. E., et al. 2005, *Nature*, 434, 50, doi: [10.1038/nature03400](https://doi.org/10.1038/nature03400)
- Kramer, M., Liu, K., Desvignes, G., Karuppusamy, R., & Stappers, B. W. 2024, *Nature Astronomy*, 8, 230, doi: [10.1038/s41550-023-02125-3](https://doi.org/10.1038/s41550-023-02125-3)
- Lo, K. K., Bray, J. D., Hobbs, G., et al. 2012, *MNRAS*, 421, 3316, doi: [10.1111/j.1365-2966.2012.20555.x](https://doi.org/10.1111/j.1365-2966.2012.20555.x)
- Lorimer, D. R. 2008, *Living Reviews in Relativity*, 11, 8, doi: [10.12942/lrr-2008-8](https://doi.org/10.12942/lrr-2008-8)
- Lorimer, D. R., Bailes, M., McLaughlin, M. A., Narkevic, D. J., & Crawford, F. 2007, *Science*, 318, 777, doi: [10.1126/science.1147532](https://doi.org/10.1126/science.1147532)
- Lynch, C. R., Lenc, E., Kaplan, D. L., Murphy, T., & Anderson, G. E. 2017, *ApJL*, 836, L30, doi: [10.3847/2041-8213/aa5ffd](https://doi.org/10.3847/2041-8213/aa5ffd)
- Marsh, T. R., Gänsicke, B. T., Hümmerich, S., et al. 2016, *Nature*, 537, 374, doi: [10.1038/nature18620](https://doi.org/10.1038/nature18620)
- McMahon, R. G., Banerji, M., Gonzalez, E., et al. 2013, *The Messenger*, 154, 35
- Norton, A. J., Wynn, G. A., & Somerscales, R. V. 2004, *ApJ*, 614, 349, doi: [10.1086/423333](https://doi.org/10.1086/423333)
- Offringa, A. R., McKinley, B., Hurley-Walker, N., et al. 2014, *MNRAS*, 444, 606, doi: [10.1093/mnras/stu1368](https://doi.org/10.1093/mnras/stu1368)

- Papitto, A., & de Martino, D. 2022, in *Astrophysics and Space Science Library*, Vol. 465, *Astrophysics and Space Science Library*, ed. S. Bhattacharyya, A. Papitto, & D. Bhattacharya, 157–200, doi: [10.1007/978-3-030-85198-9_6](https://doi.org/10.1007/978-3-030-85198-9_6)
- Parthasarathy, A., Shannon, R. M., Johnston, S., et al. 2019, *MNRAS*, 489, 3810, doi: [10.1093/mnras/stz2383](https://doi.org/10.1093/mnras/stz2383)
- Pelisoli, I., Marsh, T. R., Buckley, D. A. H., et al. 2023, *Nature Astronomy*, 7, 931, doi: [10.1038/s41550-023-01995-x](https://doi.org/10.1038/s41550-023-01995-x)
- Petroff, E., Hessels, J. W. T., & Lorimer, D. R. 2022, *A&A Rv*, 30, 2, doi: [10.1007/s00159-022-00139-w](https://doi.org/10.1007/s00159-022-00139-w)
- Rea, N., Coti Zelati, F., Dehman, C., et al. 2022, *ApJ*, 940, 72, doi: [10.3847/1538-4357/ac97ea](https://doi.org/10.3847/1538-4357/ac97ea)
- Tingay, S. J., Goeke, R., Bowman, J. D., et al. 2013, *PASA*, 30, 7, doi: [10.1017/pasa.2012.007](https://doi.org/10.1017/pasa.2012.007)
- Tody, D. 1986, in *Society of Photo-Optical Instrumentation Engineers (SPIE) Conference Series*, Vol. 627, *Instrumentation in astronomy VI*, ed. D. L. Crawford, 733, doi: [10.1117/12.968154](https://doi.org/10.1117/12.968154)
- Urry, C. M., & Padovani, P. 1995, *PASP*, 107, 803, doi: [10.1086/133630](https://doi.org/10.1086/133630)
- van Paradijs, J., Kouveliotou, C., & Wijers, R. A. M. J. 2000, *ARA&A*, 38, 379, doi: [10.1146/annurev.astro.38.1.379](https://doi.org/10.1146/annurev.astro.38.1.379)
- Vedantham, H. K., Callingham, J. R., Shimwell, T. W., et al. 2020, *Nature Astronomy*, 4, 577, doi: [10.1038/s41550-020-1011-9](https://doi.org/10.1038/s41550-020-1011-9)
- Verro, K., Trager, S. C., Peletier, R. F., et al. 2022, *A&A*, 660, A34, doi: [10.1051/0004-6361/202142388](https://doi.org/10.1051/0004-6361/202142388)
- Viganò, D., Rea, N., Pons, J. A., et al. 2013, *MNRAS*, 434, 123, doi: [10.1093/mnras/stt1008](https://doi.org/10.1093/mnras/stt1008)
- Wayth, R. B., Tingay, S. J., Trott, C. M., et al. 2018, *PASA*, 35, 33, doi: [10.1017/pasa.2018.37](https://doi.org/10.1017/pasa.2018.37)
- Willingale, R., Starling, R. L. C., Beardmore, A. P., Tanvir, N. R., & O'Brien, P. T. 2013, *MNRAS*, 431, 394, doi: [10.1093/mnras/stt175](https://doi.org/10.1093/mnras/stt175)
- Wilms, J., Allen, A., & McCray, R. 2000, *ApJ*, 542, 914, doi: [10.1086/317016](https://doi.org/10.1086/317016)
- Yao, J. M., Manchester, R. N., & Wang, N. 2017, *ApJ*, 835, 29, doi: [10.3847/1538-4357/835/1/29](https://doi.org/10.3847/1538-4357/835/1/29)